Using Coplanar Waveguides as Spin-Wave Sources with Improved Bandwidth

H. Aquino, D. Connelly, A. Orlov, J. Chisum, G. H. Bernstein and W. Porod Department of Electrical Engineering, University of Notre Dame, Notre Dame, IN, USA Email: haquino@nd.edu/Phone: (574)631-3769

Spin waves show potential as an alternative to electric current for computing and signal processing, which require low-power and small size. One approach to using spin waves is to convert millimeter or microwave electrical signals to spin waves having micrometer wavelengths. All signal processing is then done by the diffraction and interference of spin waves traveling through a magnetic thin film. These waves are then converted back into electrical signals [1,2].

Coplanar waveguides (CPW) can be used to convert electrical signals into spin waves [3]. However, because of the interference among spin waves launched from different points of the CPW, the spin-wave excitation strength from the CPW exhibits a comb-like frequency response making it unsuitable for the device described above. Taking the Fourier transform of the spatial distribution of the CPW's magnetic field (Fig. 1) gives its relative spin-wave excitation strength as a function of wavenumber [3], as shown in Fig. 2. Because the spatial frequency spectrum shown is dependent only on the spatial dimensions of the CPW, this can be designed to target a specific (temporal) frequency, but the response will always have a comb-like shape.

In order to calculate the frequency response of the launcher, it is necessary to translate the wavenumber dependence of the excitation strength to frequency using the dispersion relation of the spin-waves. The dispersion is dependent on the material parameters of the magnetic film, the magnitude and direction of the external magnetic field, and the wave vector. Despite the wavenumber response being fixed by the dimensions of the CPW, the dispersion relation can still be manipulated. While it would be impractical to manipulate the dispersion relation by changing the external DC magnetic field in a particular area, the dispersion relation can be changed under the CPW by exciting large-amplitude spin-waves using relatively high RF fields along with an out-of-plane saturating DC magnetic field. Large-amplitude spin waves have magnetizations with large angles of precession. This results in a significant change in the component of the magnetization that is parallel to the DC magnetic field, which results in a shift in the dispersion relation corresponding to longer wavelengths for the same frequencies. These wavelengths underneath the CPW conductors are considerably longer than the CPW width such that effectively no destructive interference occurs. These waves then propagate away from the CPW; as the influence of the RF field diminishes with distance, Gilbert damping lowers the amplitude of the spin waves, and a new dispersion relation becomes dominant. This new dispersion relation corresponds to that of small-amplitude spin waves that are dictated by the DC field and the saturation magnetization.

To simulate these effects, the magnetic fields of the CPW were taken from simulations in Ansys HFSS [4]. This field was added to an external DC bias field and used in Mumax3 [5] where micromagnetic simulations were done. At a low RF fields, the simulation results shown in Figs. 3, 4 and 5 were consistent with the comb-like response as predicted by the Fourier transform of the field. However, at higher RF fields, spin-waves with longer wavelength and additional unwanted spin-wave structure are launched from the CPW. These wavelengths decrease as the wave travels away from the CPW as shown in Fig. 6. We have found that placing a gap in the magnetic film after the CPW acts in the same way as a gap in a continuous magnetic yolk, *i.e.*, the magnetic field bridges the gap at the expense of losing overall field strength. This effect removes the unwanted structure and lowers the local field strength just to the right of the gap and places the spin-wave into the desired dispersion relationship, and hence the desired wavelength. With the CPW used in this way, the frequency response does not have the null of the CPW at a low RF field (Figs. 7 and 8) and is able to launch spin waves at higher frequency, as shown by the simulation results in Fig. 9 compared to Fig. 5. We see that the combination of launching large-amplitude, long-wavelength spin waves followed by a gap in the magnetic material to bring down the amplitude and wavelength of the spin wave produces a spin-wave launcher with a smooth response and wider bandwidth than using the CPW under normal conditions.

References

- [1] G. Csaba, Á. Papp and W. Porod, "Perspectives of using spin waves for computing and signal processing," *Physics Letters A*, vol. 381, no. 17, pp. 1471-1476, 2017. doi: 10.1016/j.physleta.2017.02.042
- [2] Á. Papp, W. Porod, Á. Csurgay and G. Csaba, "Nanoscale spectrum analyzer based on spin-wave interference," *Scientific Reports*, vol. 7, no. 1, 2017. doi: 10.1038/s41598-017-09485-7.
- [3] S. Maendl, I. Stasinopoulos and D. Grundler, "Spin waves with large decay length and few 100 nm wavelengths in thin yttrium iron garnet grown at the wafer scale," *Applied Physics Letters*, vol. 111, no. 1, p. 012403, 2017. doi: 10.1063/1.4991520.
- [4] "ANSYS HFSS: High Frequency Electromagnetic Field Simulation Software," Ansys.com, 2020. [Online]. https://www.ansys.com/products/electronics/ansys-hfss. [Accessed: 01- Mar- 2020].
- [5] A. Vansteenkiste, J. Leliaert, M. Dvornik, M. Helsen, F. Garcia-Sanchez and B. Van Waeyenberge, "The design and verification of MuMax3," *AIP Advances*, vol. 4, no. 10, p. 107133, 2014. doi: 10.1063/1.4899186.



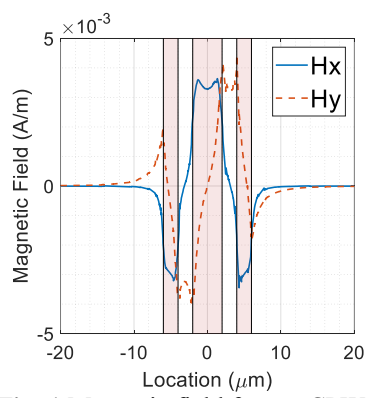


Fig. 1 Magnetic field from a CPW from HFSS.

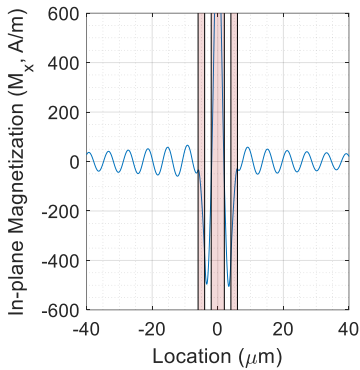


Fig. 4 f = 0.752 GHz, k = 1.05 rad/ μ m (2nd null), $\lambda = 6 \mu$ m. Note that the amplitude is roughly $1/4^{th}$ that shown in Fig. 3.

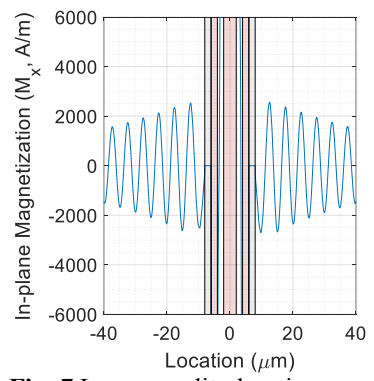


Fig. 7 Large amplitude spin-wave with a gap flush to the left and right of the CPW. f = 0.793 GHz, k = 1.29 rad/µm (2nd peak), $\lambda = 4.86$ µm.

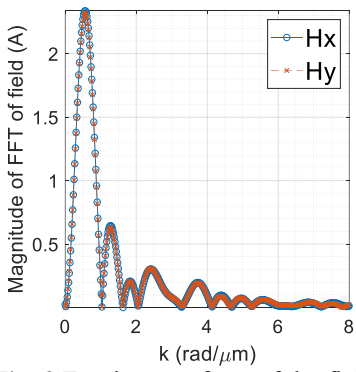


Fig. 2 Fourier transform of the field shown in Fig. 1. The FFT is proportional to the spin-wave excitation strength, and is independent of the dispersion relation and film thickness.

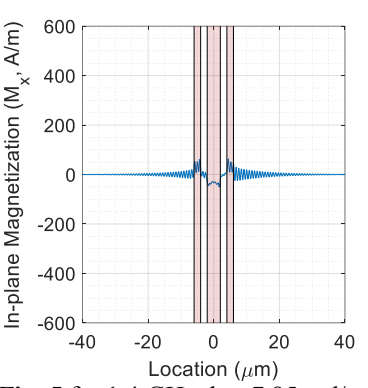


Fig. 5 f = 1.4 GHz, $k = 7.85 \text{ rad/}\mu\text{m}$ (2nd null), $\lambda = 0.8 \mu\text{m}$.

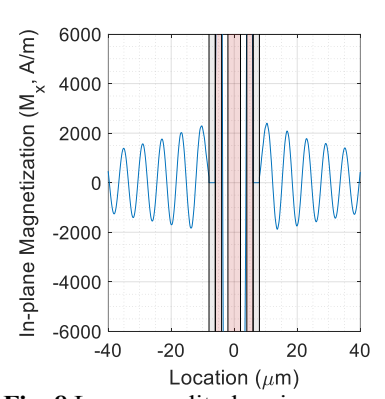


Fig. 8 Large amplitude spin-wave with a gap flush to the left and right of the CPW. f = 0.752 GHz, k = 1.05 rad/µm (2^{nd} null), $\lambda = 6$ µm, which should be a null in the frequency response.

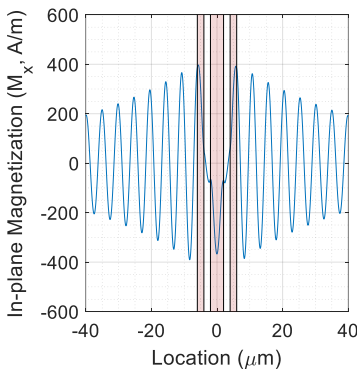


Fig. 3 Simulation results of a spin wave in a 300 nm thick YIG film with the field in Fig. 1. f = 0.793 GHz, k = 1.29 rad/ μ m (2^{nd} peak), $\lambda = 4.86$ μ m.

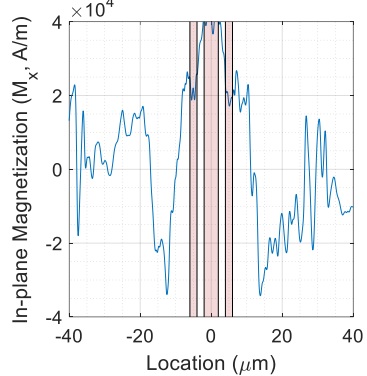


Fig. 6 Large-amplitude, long-wavelength spin waves with unwanted structure launched from a CPW. f = 0.793 GHz, k = 1.29 rad/ μ m (2^{nd} peak), $\lambda = 4.86$ μ m.

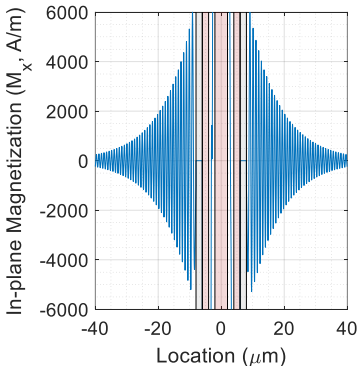


Fig. 9 Large amplitude spin-wave with a gap flush to the left and right of the CPW. f = 1.42 GHz, k = 7.85 rad/ μ m, $\lambda = 0.8$ μ m.

